Indian Journal of Pure & Applied Physics
Vol. 56, July 2018, pp. 491-508

Molecular orbital, spectroscopic, first order hyperpolarizability and NBO analysis of aryl-substituted 5-(benzylidine) thiazolidine-2,4-diones

Shaheen Fatma[a], Huda Parveen[a], Abha Bishnoi[a]*, Anil Kumar Verma[a] & Krishna Srivastava[b]

[a]Department of Chemistry, University of Lucknow, Lucknow 226 007, India

[b]Department of Chemistry, Shri Ramswaroop Memorial University, Lucknow 226 001, India

Received 3 July 2017; accepted 26 December 2017

In this study, the structure of three 5-(4-subs/3, 4- di substituted benzylidene) thiazolidine-2,4-diones has been studied by using density functional theory (DFT) at 6-31G(d,p) level basis set. Detailed interpretations of the vibrational spectra of these compounds have been made on the basis of the calculated potential energy distribution (PED). The ^{1}H and ^{13}C NMR spectra have been recorded and the chemical shifts have been calculated using the gauge- independent atomic orbital method (GIAO). The values of frontier orbital energy gap (-3.64 eV) and dipole moment (4.7012 D) show that the compound 3b is less reactive and less polar, hence the most stable among the three molecules. The significantly higher value (131.96×10^{-30} esu) of total hyperpolarizability for compound 3c indicates the better use of this molecule as NLO material. The calculated local reactivity descriptors for 3(a-c) indicate that C2 is the most reactive site for nucleophilic attack whereas the oxygen attached to this C is more prone to electrophilic attack. Hyperconjugative interactions have been studied with the help of natural bond orbital analysis. The electronic properties and thermodynamic properties have also been performed.

Keywords: Density functional theory (DFT), Natural bond orbital (NBO), Non linear optical (NLO), Molecular electrostatic potential (MESP), Hyperpolarizability

1 Introduction

Thiazolidinediones (TZDs), also referred to as glitazones, act as a potent antidiabetic agents targeting nuclear receptor, peroxisome proliferator-activated receptor-γ (PPARγ), as potent inhibitors of PI3Kγ[1], Pim kinase family[2], and HIV-1 entry protein gp41[3] also exhibiting their versatile roles in multiple indications spanning from inflammatory diseases to cancers. FDA approved several TZDs for treating type 2 diabetes[4] and has a weaker influence on vulcanizing rate[5]. Improvement in the qualities of photosensitizing composition has been reported by the addition of thiazolidine-2,4-dione and some of their derivatives to photosensitizing compositions[6,7]. These are also small molecule inhibitors of numerous biological targets including aldose reductase[8], 15 hydroxyprostaglandin dehydrogenase[9] and enzyme MurD ligase[10]. Furthermore, TZDs showed various biological activities such as antihyperglycemic[11], bactericidal[12], pesticidal[13], fungicidal[14], insecticidal[15], anticonvulsant[16], tuberculostatic[17] and anti-inflammatory[18].

The present paper deals with the detailed spectroscopic analysis, non linear optical properties (NLO), thermodynamic properties, Molecular electrostatic potential (MEP) and chemical reactivities of some of the 5-(4-subs/3,4- di substituted benzylidene)thiazolidine-2,4-diones by quantum chemical calculations. The redistribution of electron density (ED) in various bonding and antibonding orbitals and E(2) energies were calculated by natural bond orbital (NBO) analysis to give clear evidence of stabilization originating from the hyperconjugation of various intra-molecular interactions. Detailed interpretations of the vibrational spectra of the molecules have been made, based on the calculated potential energy distribution[19] (PED).

2 Materials and Method

The FTIR spectrum was carried out between 4000 cm^{-1} and 400 cm^{-1} on Bruker Tensor -27 FTIR spectrometer using the KBr pellet technique. ^{1}H- and ^{13}C-NMR (Nuclear Magnetic Resonance) spectra were recorded on Bruker 300 MHz instrument using DMSO as a solvent. Chemical shifts are reported in parts per million (p.p.m.) using tetramethylsilane (TMS) as an internal standard. The positive electron spray ionization (ESI) high resolution mass spectrometry of compound 3c was recorded on Agilent 6520(Q-TOF) mass spectrometer and the

*Corresponding author (E-mail: abhabishnoi5@gmail.com)

DART-MS of compound 3a and 3b was recorded on JEOL-AccuTOF JMS-T1100LC Mass spectrometer having a DART (Direct Analysis in Real Time) source. The sample was subjected as such in front of DART source. Dry Helium was used with 4LPM flow rate for ionization at 350 °C. Ultra violet (UV) spectra were recorded on UV- visible double-beam spectrophotometer (systronic-2203) instrument using ethanol for compound 3c and DMSO as a solvent for compound 3a and 3b. Melting points were determined in a melting point apparatus and are uncorrected. Potential energy distribution along with internal coordinates is calculated by Gar2ped software[20]. All solvents used were of laboratory grade and were purified and dried according to standard procedures prior to their use. Thin layer chromatography (TLC) on Silica Gel coated plates were used for monitoring the progress of reaction and purity of the compounds and were visualized in an iodine chamber.

2.1 Synthesis of 5-(3-hydroxy, 4-methoxy /4-methoxy /4-N,N-dimethylbenzylidene) thiazolidine-2,4-diones (3a-c)

The synthetic route for compounds (3a-c) is illustrated in Scheme 1. Piperidine was added to a suspension of thiazolidine- 2,4-dione(1) and substituted benzaldehyde (2) in EtOH, and the reaction mixture was refluxed for about 5-8 h. The progress of the reaction was monitored by TLC. The precipitate, separated on cooling the reaction mixture, was filtered, washed with water and recrystallised with ethanol[21].

3 Computational Methods

Quantum chemical calculations for all the compounds were carried out with 3-parameter hybrid functional[22,23] (B3) for exchange part and the Lee-Yang-Parr[24] (LYP) correlation function, with 6-31G(d,p) as the basis set using[25] the GAUSSIAN 09 suite of program and results were analyzed with the Gaussview 5.0 molecular visualization program[26]. The assignments of the calculated normal modes have been made on the basis of the corresponding PEDs.

4 Results and Discussion

4.1 Molecular geometry

The optimized structure along with the atoms numbering scheme of compounds 3(a-c) at DFT/B3LYP level using the 6-31G (d, p) basis set are shown in Fig. 1. The C-H/aromatic C-C bond lengths vary in the range 1.080 Å-1.096 Å/1.383 Å-1.417 Å/, 1.084 Å-1.096 Å/1.380 Å-1.417 Å and 1.081 Å-1.097 Å/1.381 Å-1.418 Å (standard value 1.10 Å/1.40 Å), respectively, in 3a, 3b and 3c. The alkenic / thiazole C-C bond lengths have been found at 1.361/1.486 Å, 13.616/1.4822 Å, 1.364/ 1.4775 Å in 3a, 3b and 3c, respectively. The C=O bond lengths (C is directly attached to C and N)/ C=O (C is directly attached with N and S) for three molecules are calculated to be 1.221 Å/1.206 Å, 1.221 Å/1.206 Å and 1.2231 Å/1.207 Å, respectively, which are close to the standard range[27] 1.196 to 1.211 Å. The C-O bond length is found to be larger than usual C-O bond length[28] due to the shifting of electron cloud from C atom to O atom for 3a (1.2231 Å). The C–S/N-H bond lengths are found to be very close to the C-S bond distance[29] and N-H bond distance and are 1.798/1.012, 1.798/1.012, 1.800/1.012 Å respectively for 3a, 3b and 3c. In general optimized parameters agree very well with the available experimental XRD data[30-34].

4.2 ^{1}H NMR and ^{13}CNMR spectroscopy

For the structural analysis of organic compounds, chemical shift analysis is one of the most important techniques. ^{1}H and ^{13}C NMR chemical shifts calculations of optimized molecules were carried out by using GIAO method and B3LYP functional with 6-31G (d,p) basis sets. The experimental and calculated values of ^{1}H and ^{13}C NMR chemical shifts are given in Table 1 and Table 2, respectively.

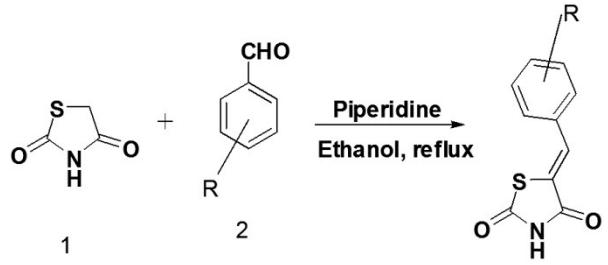

Compound	R
3a	-3-hydroxy-4-methoxy
3b	-4-methoxy
3c	-4-N,N-dimethyl

Scheme-1

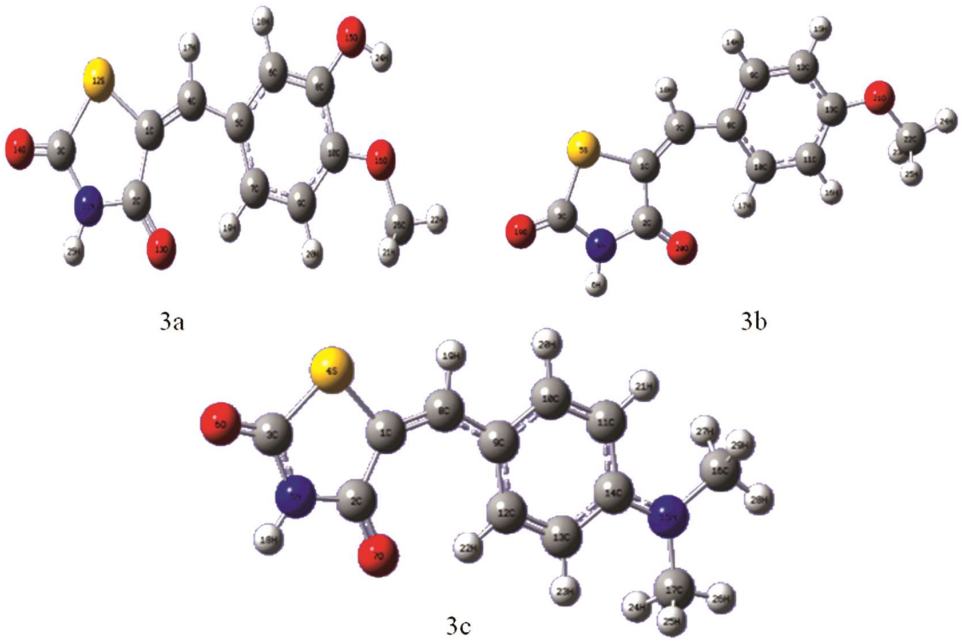

Fig. 1 — Optimized geometries of the compounds 3(a-c) using B3LYP/6-31G (d, p) level of theory.

Table 1 — Experimental and calculated ^{1}H chemical shifts for compounds 3(a-c) using B3LYP with 6-31G/(d, p)basis set.

Atom No (3a)	B3LYP	Experimental	Atom No (3b)	B3LYP	Experimental	Atom No (3c)	B3LYP	Experimental
H17	6.70	7.62	H6	7.60	12.47	H18	6.93	3.34
H18	6.80	7.02	H14	7.68	7.05	H19	6.57	7.65
H19	9.56	7.08	H17	9.99	7.08	H22	9.80	7.39-7.42
H20	6.98	7.04	H15	7.40	7.51	H20	7.19	
H21	3.87	3.82	H16	7.58	7.54	H21	6.69	6.78-6.81
H22	4.21	3.82	H18	7.56	7.72	H23	6.72	
H23	3.87	3.82	H23	4.38	3.81	H24	3.26	3.006
H24	5.53	9.48	H24	4.64	3.81	H25	3.27	3.006
H25	7.04	12.45	H25	4.38	3.81	H26	2.85	3.006
						H27	3.25	3.006
						H28	2.85	3.006
						H29	3.25	3.006

Table 2 — Experimental and calculated ^{13}C chemical shifts for compounds 3(a-c) using B3LYP with 6-31G/(d, p)basis set.

Atom No (3a)	B3LYP	Experimental	Atom No (3b)	B3LYP	Experimental	Atom No (3C)	B3LYP	Experimental
C1	125.65	115.94	C1	159.93	120.27	C1	120.06	115.67
C2	160.03	167.44	C2	160.39	167.92	C2	159.53	167.56
C3	164.94	168.08	C3	160.09	167.41	C3	165.18	168.18
C4	142.16	132.29	C7	145.91	131.79	C8	141.56	132.93
C5	125.95	125.7	C8	138.39	125.47	C9	121.12	119.81
C6	119.82	120.43	C9	145.53	132.04	C10	136.88	132.14
C7	124.08	123.47	C10	145.76	132.04	C11	109.79	112.04
C8	143.74	146.96	C11	121.01	114.86	C12	131.78	132.14
C9	109.81	112.41	C12	128.36	114.86	C13	110.42	112.04
C10	148.73	150.05	C13	175.16	160.95	C14	148.08	151.45
C26	56.65	55.68	C22	59.37	55.44	C16	43.36	40.34
						C17	43.49	40.34

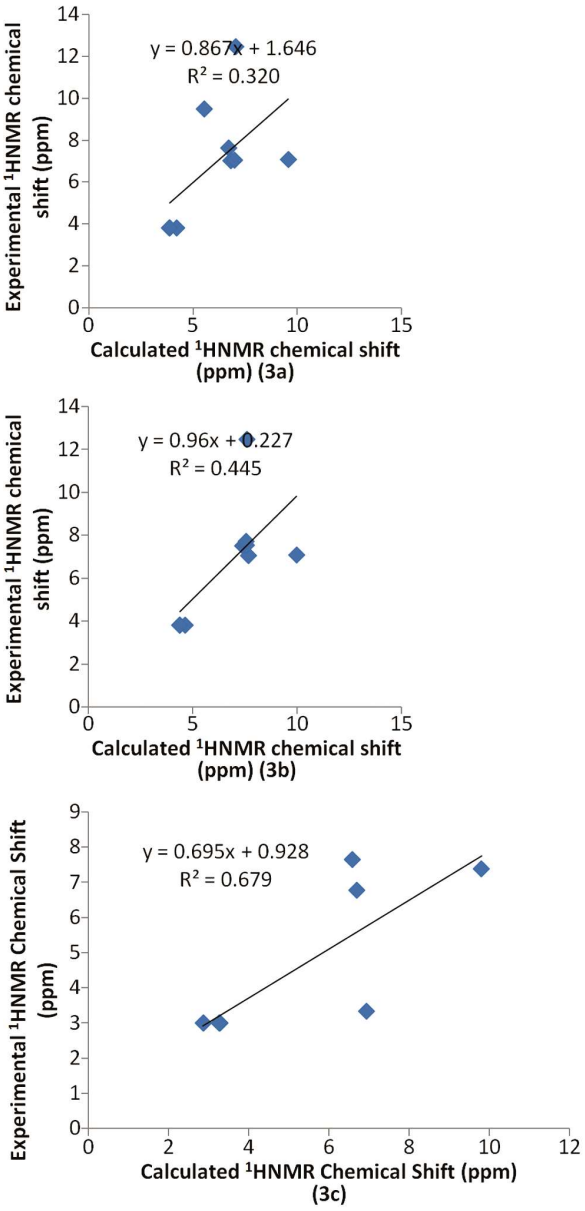

Fig. 2 — Correlation graph between experimental and calculated ^{1}HNMR chemical shift for compounds 3(a- c) using B3LYP /6-31G (d, p).

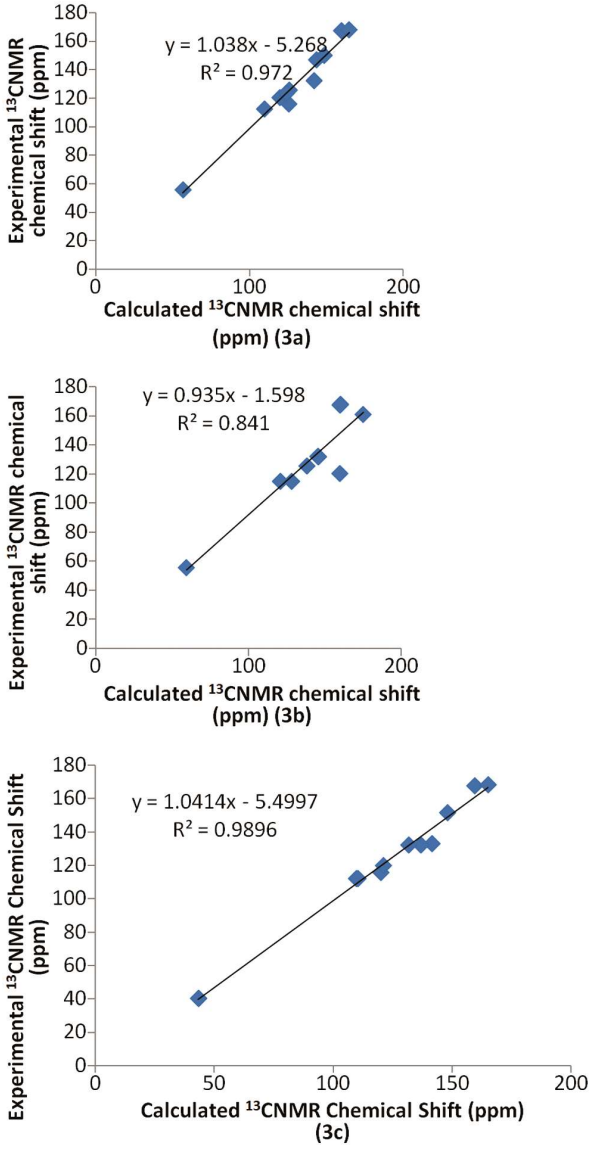

Fig. 3 — Correlation graph between experimental and calculated ^{13}CNMR chemical shift for compounds 3(a- c) using B3LYP with the basis set 631-G(d,p).

Agreement between theory and experiment is inconsistent: sometimes good, sometimes poor. Both, experimental and theoretical results are in agreement except for the proton of the NH group in case of ^{1}HNMR of compound[35] 3c. The correlation graphs between the experimental and calculated chemical shifts for ^{1}H and ^{13}C NMR are shown in Fig. 2 and Fig. 3, respectively.

4.3 UV-Visible absorption spectroscopy

The electronic spectrum was recorded within the range 190–600 nm in DMSO for compounds 3a and 3b and in ethanol for compound 3c. Electronic absorption wavelengths, excitation energies, oscillator strengths were calculated by the TD (DFT)/B3LYP/6-31G (d,p) level and solvent effect has been taken into consideration by implementing Integral Equation Formalism Polarizable Continuum Model (IEFPCM) are listed in Table 3. The calculated values correspond well with the experimental data. Numerous applications for the use of the HOMO–LUMO gap as a quantum descriptor in establishing correlation in various chemical and biological systems are available. Calculations obtained by B3LYP functional are in good agreement with the measured experimental data.

Table 3 — Experimental and theoretical absorption wavelength λ (nm), excitation energies *E* (eV) of title compounds 3(a-c) using B3LYP functional and 6-31G/(d,p) basis set.

	Electronic transitions (molecular orbitals involved)	Energy (ev)	Calculated λ_{max} (in nm)	Oscillatory strength (*f*)	Percent contribution of probable transition B3LYP	Observed λ_{max} (in nm)
Compound 3a						
	(H-1)-L	4.275	390.41	0.4919	1.337	396
	H-L	3.5072			48.5	
Compound 3b						
	H-L	3.3537	369.69	0.7655	49.85	352
Compound 3c						
	H-L	3.21	410.7	0.9031	50.01	378
	(H-5)-L	6.08	295.96	0.001	1.6	242

All these transitions appear to be due to $\pi \pi^*$ transition. The calculated frontier orbital gaps for 3a/ 3b/3c are 3.5072/3.6334 /3.217 eV respectively. 3c having low value of frontier orbital gap is highly polarizable and has high chemical reactivity, low kinetic stability and could be termed as soft molecule[36]. Molecular orbitals of compounds and their electronic transitions are shown in Fig. 4(a-c), exhibiting the distributions and energy levels. Figure 4(a) shows that HOMO-1 is delocalized over the whole of the molecule except NH and OCH_3 group, LUMO is delocalized over whole of the molecule except OH, S atom and the methyl group of methoxy moiety. Figure 4(b) shows that HOMO is delocalized over whole of the molecule except methyl group of methoxy moiety and LUMO is delocalized over whole of the molecule except NH group. Figure 4(c) shows that HOMO is localized over whole molecule except the NH group of thiazolidinone moiety, HOMO – 5 is delocalized only on thiazolidinone ring and LUMO is localized over whole of the molecule except S atom and methyl group of dimethylamino moiety, showing the chemical reactivity and occurrence of eventual charge transfer within the molecule.

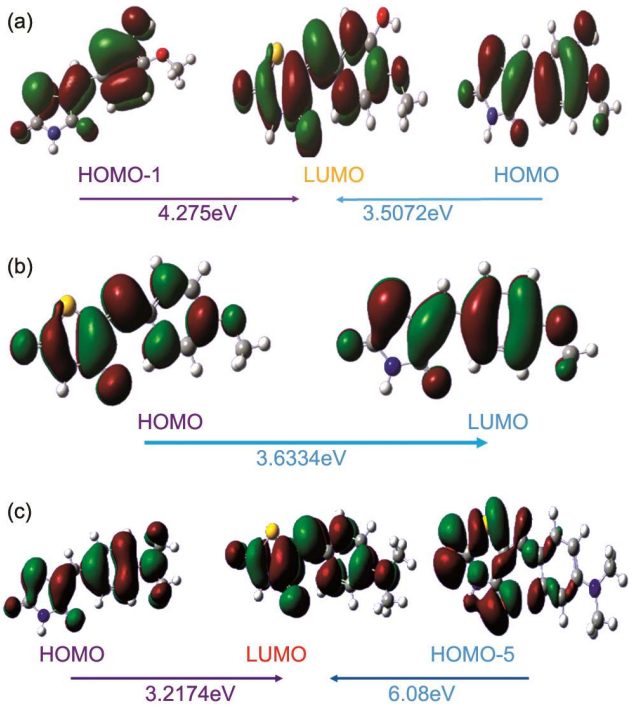

Fig. 4 — (a) Molecular orbitals of the compound 3a at the B3LYP/ 6-31G(d, p) basis set, (b) molecular orbitals of the compound 3b at the B3LYP/ 6-31G(d, p) basis set and (c) molecular orbitals of the compound 3c at the B3LYP/ 6-31G (d, p) basis set.

4.4 Vibrational assignment

Since the compounds 3a, 3b and 3c consist of 26, 25 and 29 atoms, respectively, therefore they have 72, 69 and 81 fundamental vibrations. Since the computations were performed for isolated molecules in the gas phase and the measurements were recorded in the solid phase, the calculated harmonic vibrational wavenumbers become greater than the observed vibrational wavenumbers due to the states such as negligence of anharmonicity, electron correlation and basis set deficiencies[37,38]. For this reason, in order to compare the calculated and observed vibrational wavenumbers, vibrational frequencies calculated at B3LYP/6-31G (d,p) level were scaled by the typical factor[39] 0.9679. DFT based calculations are a good source for understanding the energy distribution of each vibrational mode on the basis of potential energy distribution (PED) and lead to an additional interpretation of the vibrational spectroscopic data for molecules[40-43]. The recorded (FTIR) and computed vibrational wavenumbers by B3LYP/6-31G(d,p), IR activities along with the assignments of vibrational modes of compound based on PED results are given in Table 4(a-c).

Table 4(a) — The recorded (FTIR) and computed vibrational wavenumbers by B3LYP/6-31G(d,p), IR activities along with the assignments of vibrational modes of compound 3a based on PED results.

	Theoretical wavenumber				
	Unscaled	Scaled	Experimental	I_{IR}(km/mol)	Vibrational assignment (PED in %)
28	678.58	656.7976	630.7	66.66	ν(C3-S12)(42.), β(N11-O14-C3)(15.), β(C1-O13-C2)(11)
41	1140.08	1103.483	1016.45	861.77	ν(C3-N11)(25.), -ν(C2-N11)(18.), -
43	1175.25	1137.524	1134.10	1.17	β(H21-O16-C26)(70.), β(H22-O16-C26)(24.),
48	1297.79	1256.131	1213.18	974.5	ν(C10-O16)(17.), -β(C1-O13-C2)(13.),
49	1307.82	1265.839	1244.04	225.48	ν(C8-O15)(12.),
51	1377.74	1333.515	1363.62	79.3	ν(C5-C7)(22.),
56	1497.96	1449.875	1438.84	1.48	β(C9-H19-C7)(18.), -ν(C7-C9)(15.), ν(C5-C7)(14.),
58	1555.66	1505.723	1460.06	519.42	β(C10-H20-C9)(18.), -ν(C8-C10)(13.), -β(C5-H18-C6)(12
59	1600.42	1549.047	1510.21	452.7	ν(C1-C4)(25.), -ν(C4-C5)(11
60	1629.62	1577.309	1587.36	80.73	ν(C1-C4)(14.), ν(C9-C10)(13)
62	1753.6	1697.309	1691.51	749.45	ν(C2-O13)(52.), -β(S12-C2-C1)(16.), -ν(C3-O14)(11.),
63	1801.3	1743.478	1733.94	1016.08	ν(C3-O14)(67.), ν(C2-O13)(12.),
64	3044.33	2946.607	2783.18	87.19	ν(H23-C26)(44.), ν(H21-C26)(44.),
65	3117.79	3017.709		37.62	ν(H21-C26)(50.), -ν(H23-C26)(50.),
66	3145.84	3044.859	3024.27	11.38	ν(C4-H17)(99.),
70	3261.41	3156.719	3126.5	45.95	ν(C7-H19)(97.),
71	3609.96	3494.08	3435.1	159.62	ν(N11-H25)(99.),
72	3755.06	3634.523	3531.53	176.03	ν(O15-H24)(100.),

Table 4(b) — The recorded (FTIR) and computed vibrational wavenumbers by B3LYP/6-31G(d,p), IR activities along with the assignments of vibrational modes of compound 3b based on PED results.

	Theoretical wavenumber				
Mode	Unscaled	Scaled	Experimental	I_{IR}(km/mol)	Vibrational assignment (PED in %)
32	860.16	832.5489	831	13.23	ν(C1-S5)(11.), -β(S5-C2-C1) 11.), β(C10-C9-C8) 11.),
38	1070.15	1035.798	1014.52	67.57	ν(O21-C22)(75.),
39	1142.36	1105.69	1182.32	270.83	ν(C3-N4)(32.), -ν(C2-N4)(18.),
44	1248.89	1208.801	1419.55	38.21	ν(C7-C8)(23.), -ν(C10-C11)(13.),
48	1364.77	1320.961	1454.27	66.28	ν(C8-C10)(21.), ν(C11-C13)(13.), -ν(C8-C9)(10.),
51	1476.16	1428.775	1508.28	46.62	ν(C9-C12)(23.), -ν(C10-C11)(17.),
55	1556.47	1506.507	1593.14	120.27	β(C8-H14-C9) 17.), ν(C12-C13)(12.), β(C8-H17-C10) 10.)
56	1602.42	1550.982	1593.14	34.53	ν(C11-C13)(15.), -ν(C8-C10)(15.), -ν(C12-C13)(14.), ν(C1-C7)(12.),
59	1782.88	1725.65	1701.15	245.8	ν(C2-O20)(63.), -β(S5-C2-C1)(14.),
60	1843.31	1784.14	1735.87	727.05	ν(C3-O19)(78.),
61	3026.05	2928.914	2854.54	63.59	ν(C22-H23)(45.), ν(C22-H25)(45.), ν(C22-H24)(10.),
63	3135.02	3034.386	3012.7	6.5	ν(C7-H18)(99.),
64	3157.85	3056.483		24.42	ν(C22-H24)(90.), -ν(C22-H25)(5.),
65	3183.36	3081.174	3234.51	9.63	ν(C9-H14)(93.), -ν(C12-H15)(6.),
66	3217.2	3113.928	3234.51	7.51	ν(C12-H15)(93.), ν(C9-H14)(5.),
67	3223.02	3119.561	3234.51	8.97	ν(C11-H16)(95.), -ν(C10-H17)(3.),
68	3250.74	3146.391	3234.51	29	ν(C10-H17)(96.), ν(C11-H16)(3.),
69	3624.11	3507.776	3427.38	91.67	ν(N4-H6)(99.),

Proposed assignment and potential energy distribution (PED) for vibrational modes: types of vibrations: ν – symmetric stretching; νas asymmetric stretching; β – in-plane bending; βasy – asymmetric in-plane- bending; π – out-of-plane bending; δ – linear bend; τ - torsio τasy – asymmetric torsion

Table 4(c) — The recorded (FTIR) and computed vibrational wavenumbers by B3LYP/6-31G(d,p), IR activities along with the assignments of vibrational modes of compound 3c based on PED results.

Mode	Theoretical wavenumber Unscaled	Scaled	Experimental	I_{IR} (km/mol)	Vibrational assignment (PED in %)
24	590.92	571.95147	505	109.97	π(C20-C9-C11)(80.), πasy(O6-S4-N5-C3) (7.), τasy(C1-C8)(6.).
25	615.81	596.0425	597.5	55.98	β(C1-N5-C2) 48.), δasy(S4-C8-C1-C9)(10.), β(S4-C2-C1)(9.), ν(C2-N5) (7.), ν(C3-N5) (7.), ν(C1-S4) (7.).
26	641.8	621.19822	605	50.86	π(O6-S4-N5-C3) (56.), τ(C1-C2) (23.), π(C20-C9-C11)(15.).
27	647.06	626.28937		17.85	β(C9-C11-C10) (64.), , ν(C3-S4) (7.), βasy(C1-N5-C2) (3.).
28	681.5	659.62385	630	86.15	ν(C3-S4) (43.), βasy(S4-O6-C3) 15.), βasy(N5-C7-O2) 13.), ν(C1-C2) 6.), βasy(C9-C11-C10) 4.), ν(C2-N5) (3.),
36	939.61	909.44852		10.33	δ(H19-C9-C8-C12)(62.), τ(C1-C8)(33.).
37	961.49	930.62617	900	26.9	ν(N15-C16)(26.), ν(N15-C17) 25.), νasy(C13-C14) 9.),
40	1000.79	968.66464	950	109.88	ν(C1-S4) (19.), δasy(S4-C8-C1-C9)(18.), δ(C1-C9-C8-C10) 17.), νasy(C1-C2) 13.),
48	1225.87	1186.5196		646.08	β(C9-H20-C10) (27.), βasy(C10-H21-C11) (9.), β(C9-H22-C12) (9.),
49	1268.38	1227.665	1190	188.83	ν(C8-C9) (14.), βasy(C12-H23-C13) (14.), νasy(C12-C13) (10.),
50	1273.76	1232.8723	1225	34.61	ν(N15-C17) (19.), νasy(N15-C16) (18.), β(C10-H21-C11) (11.),
52	1362.66	1318.9186	1318	75.46	β(C9-H22-C12) (21.), β(C12-H23-C13) (14.), νasy(C8-C9) (12.), ν(C9-C12) (10.),
55	1403.09	1358.0508	1340	1054.13	ν(C14-N15) (36.), βasy(H29-H27-C16) (9.),
56	1439.71	1393.4953	1380	448.88	δ(H19-C9-C8-C12)(37.), ν(C1-C8) (12.), νasy(C1-C2) (11.),
58	1487.13	1439.3931	1437.5	296.36	ν(C10-C11) (21.), βasy(H29-H27-C16) (20.), βasy(C10-H21-C11) (16.),
65	1574.37	1523.8327	1525	68.44	ν(C9-C12) (20.), νasy(C13-C14) (16.), ν(C14-N15) (14.),
66	1598.29	1546.9849	1570	1060.16	ν(C1-C8) (24.), ν(C9-C10) (12.), νasy(C8-C9) (11.), ,
67	1668.25	1614.6992	1612.5	360.99	ν(C10-C11)(20.), ν(C12-C13) (17.), ν(C1-C8) (12.),
68	1743.04	1687.0884	1684	768.3	ν(C2-O7) (52.), βasy(S4-C2-C1)(15.), νasy(C3-O6) (9.), νasy(C1-C2) (4.),
69	1792.44	1734.9027	1725	1119.45	ν(C3-O6) (69.), ν(C2-O7) (9.), νasy(C3-N5) (9.), βasy(C1-N5-C2) (8.).
72	3076.96	2978.1896	2770(sym)	36.3	ν(C16-H29) (50.), νasy(C16-H27) (49.).
73	3078.03	2979.2252	2825 (asy)	55.02	ν(C17-H25) (50.), νasy(C17-H24) (49.).
74	3139.8	3039.0124	3001.13	12.03	ν(C8-H19) (99.).
75	3160.56	3059.106		3.85	ν(C16-H28) (46.), νasy(C17-H26)(45.),
76	3171.29	3069.4916		45.42	ν(C17-H26)(47.), ν(C16-H28) 46.).
77	3182.01	3079.8675	3030.06	18.19	ν(C10-H20) (97.),
78	3227.99	3124.3715		12.73	ν(C13-H23) (91.), νasy(C12-H22) (8.).
79	3235.17	3131.321		20.07	ν(C11-H21)(97.).
80	3248.16	3143.8941		40.62	ν(C12-H22) (92.), ν(C13-H23) (7.).
81	3610.96	3495.0482	3498.75	157.08	ν(N5-H18) (99.).

Proposed assignment and potential energy distribution (PED) for vibrational modes: types of vibrations: ν – symmetric stretching; νasy- asymmetric stretching; β – in-plane bending; βasy – asymmetric in-plane- bending; π – out-of-plane bending; δ – linear bend; τ - torsion ; τasy – asymmetric torsion

The correlation coefficient values (R^2= 0.997, 0.9844 and 0.997 for compounds 3a, 3b and 3c) showed that there is good agreement among the scaled values of the computed harmonic frequencies and the observed ones**.** The correlation graph is shown in Fig. 5. The experimental and theoretical IR spectra for compounds 3(a-c) are given Fig. 6.

4.4.1 OH Vibrations

The strong band calculated at 3531.53 cm^{-1} in IR spectra of 3a shows the presence of OH group. These bands contribute 100% to the total[44] PED (experimental value 3634.52 cm^{-1}). The small discrepancy between the calculated and the observed wavenumber may be due to the intramolecular hydrogen bond interaction between O16….H25 as predicted by AIM (shown in Fig. 9).

4.4.2 N-H Vibrations

For heterocyclic molecules, the position of N-H stretching band depends upon the degree of hydrogen bonding and is observed in the range[45] of 3500-3200 cm^{-1}. The N-H stretching is calculated at 3494.08 /3507.77/3495.04 cm^{-1} for 3a/3b/3c while the

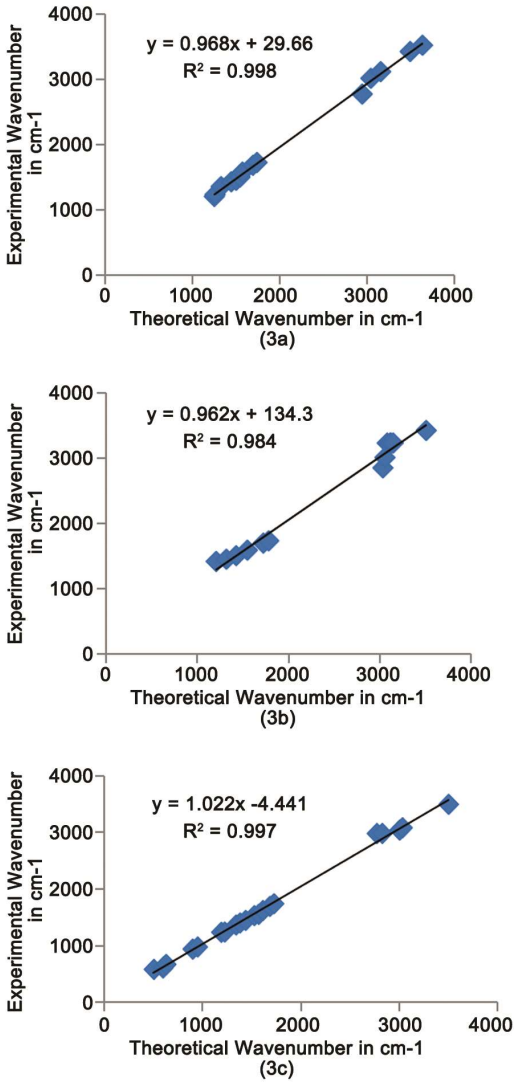

Fig. 5 — Correlation graph between experimental and calculated wavenumbers using B3LYP /6-31G (d, p) for compound 3a, 3b and 3c.

corresponding observed mode is at 3435.10 / 3427.38 / 3498.75 cm^{-1}.

4.4.3 Phenyl ring vibration

The aromatic C–H stretching vibrations are a collection of weak-to-moderate bands in the region[46] between 3100 and 3000 cm^{-1}. A strong band at 3126.5, 3234.51 and 3030.06 cm^{-1} in FTIR of compounds 3a, 3b and 3c are assigned to aromatic =C–H ring stretching vibrations, these bands show best agreement with the predicted values at 3156.71, 3146.39 and 3079.86 cm^{-1} for compounds 3a, 3b and 3c, respectively. A Band at 3024.27, 3012.7 and 3001.13 cm^{-1} in FTIR spectra of compounds is assigned to alkenic =C–H ring stretching vibrations, and are in best agreement with the predicted values at 3044.85, 3034.38 and 3039.01cm^{-1}. In aromatic compounds, in-plane C-H bending vibrations classically occur in the region[47] 1150–950 cm^{-1}. The aromatic C–H in-plane bending modes of benzene and its derivatives are observed in the region[48] 1300–1000 cm^{-1}. The C-H in-plane bending vibration for compound 3a/3b and 3c are found at 1505.72/1506.50 and 1318.91 and are well matched with experimentally observed bands at 1460.06/1593.11 and 1318 respectively in FTIR spectra. The C–H out of plane bending modes and torsional vibrations appear in general in the low-wave-number regions. In experimental FTIR spectra, the stretching modes for C=C vibration appeared at 1587.36, 1510.21, 1438.84, 1363.62 cm^{-1} /1508, 1454.27 / 1612.5, 1570, 1525, 1437.5, 1380 cm^{-1} for compound[49] 3a/3b/3c**.**

4.4.4 Methyl group vibrations

The C–H asymmetric and symmetric stretching vibrations have been reported at 3005, 2982 and 2958 and 2937 cm^{-1} by Subramanian *et. al.*[50] Arjunan *et. al.*[51] reported C-H stretching modes at 2924 cm^{-1}. The anti-symmetric C–H and symmetric stretching mode of CH_3 are computed at 3071.96 (87%), 3017.70 (50%), 2946.60 (44%) / 3056.48 (90%), 2993.09 (50%), 2928.91 (45%) / 3069.49 (26%), 3059.10 (26%), 3039.01 (50%), 2932.30 (46%), 2925.23 (47%) cm^{-1} for compound 3a/3b/3c show good agreement with experimental observations at 2783.18/ 2854.54/ /2825 (asy), 2770(sym) cm^{-1}.

4.4.5 C=O stretching

The C=O stretch of aldehyde group in 3a/ 3b/ 3c is calculated to be at 1697 (52%) and 1743.47 (67%)/1725.65 (63%) and 1784.65 (78%) /1687.08 (52%) and 1734.90 (69%) cm^{-1} and is assigned well with the experimental IR peak[52] at 1733.94 and 1691.51 cm^{-1}/1735.87 and 1701.15/ 1725 and 1684 cm^{-1}. The other strong bands observed at 1244.04 and 1213.18 cm^{-1}/ 1014.52 cm^{-1} for 3a/3b is due to C-O stretching vibration of the (C-OH and C-OCH_3) bond whose general position[53,54] is 1000-1200 cm^{-1}. This band is calculated at 1265.83 (17%) and 1256.13(12%) cm^{-1}/ 1035.79 (75%) cm^{-1} for compound 3a/3b. The C-O-C stretching vibrations reported by Klimentova *et al.*[55] lie in the range at 1214–1196 cm^{-1} and 1097-1093 cm^{-1}.

4.4.6 C-S vibrations

The C-S stretching in 3a/ 3b/ 3c is calculated to be at 656.79/832.54/968.66 cm^{-1} and is assigned well with the experimental IR peak[56] at 630.7 / 831 / 950 cm^{-1}.

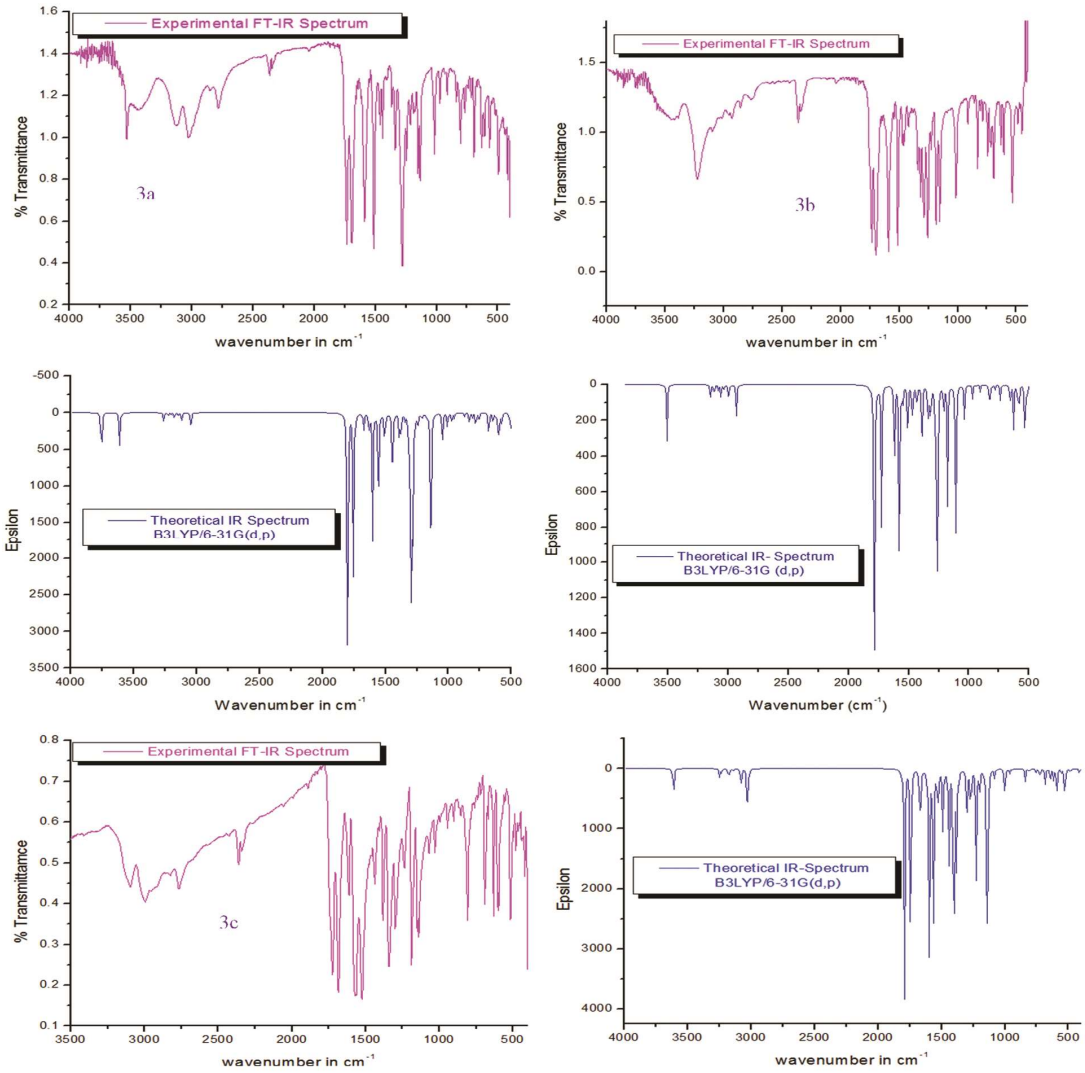

Fig. 6 — Experimental and theoretical IR spectra of compound 3(a-c).

4.4.7 C-N vibrations

Sundaraganesan *et al.*[57] assigned the band at 1302 cm^{-1} to C–N stretching vibration. Krishna Kumar and Ramasamy[58] have assigned C-N stretching mode at 1256 cm^{-1}. Referring to the above workers, the C-N stretching band is assigned at 1016.45/ 1182.32/ 1340 and 1225 cm^{-1}. The observed peak agrees well with the theoretically calculated values at 1103.48/ 1105.69 / 1358.05 and 1232.87.

4.5 Molecular electrostatic potential

To predict reactive sites for the electrophilic and nucleophilic attack, the molecular electrostatic potential (MEP) was calculated at B3LYP/6-31+G (d, p). Potential decreases in the order red < orange < yellow < green < blue showing red as most electro negative MEP, blue as most positive MEP and green as the region of zero potential. The MEP surface provides necessary information about the reactive sites. The total electron density onto which the electrostatic potential surface has been mapped is shown in Fig. 7. The negative regions were related to electrophilic reactivity and the positive ones to nucleophilic reactivity. Figure 7, provides a visual representation of the chemically active sites and comparative reactivity of atoms[59]. The major positive potential region around hydrogen atom of thiazolidinone moiety characterized by blue colour indicates the site for nucleophilic attack and major negative potential region around oxygen atom of carbonyl group characterized by yellowish red indicate that this site is more prone to electrophilic attack while rest of the region is almost neutral characterized by blue colour.

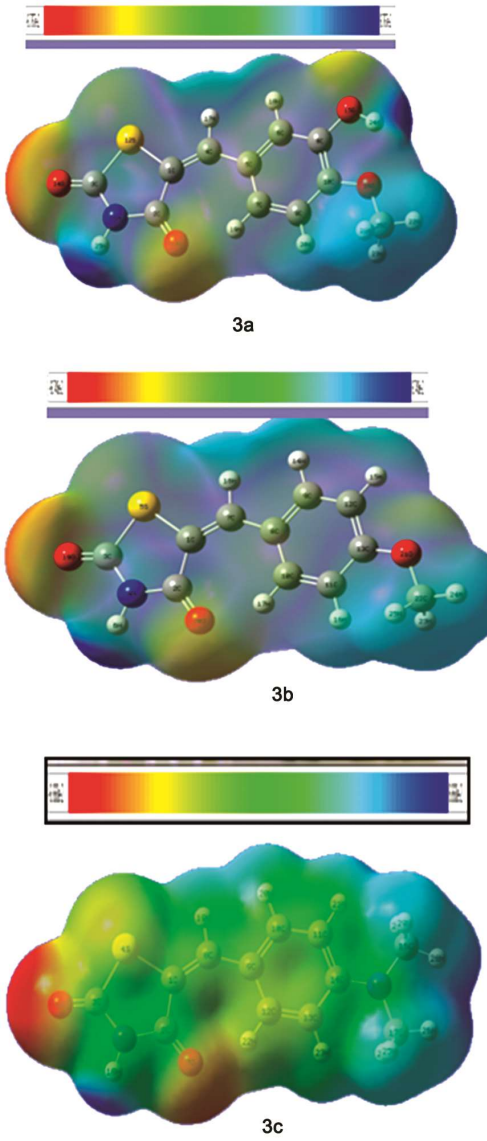

Fig. 7 — 3D plots of the molecular electrostatic potentials of 3(a-c).

4.6 Natural bond orbital analysis

A useful aspect of the NBO method is that it gives information about interactions in both filled and virtual orbital spaces that could enhance the analysis of intra- and intermolecular interactions. The second-order Fock matrix was calculated to evaluate the donor–acceptor interactions in NBO analysis.

The Natural Bond Orbital (NBO) calculations[60] were performed using Gaussian09 package at the B3LYP/6-31G (d, p) method in order to elucidate the intramolecular, rehybridization and delocalization of electron density in the molecule and were presented in Table 5(a-c). Various intra and intermolecular interactions are generated due to the different types of ‘‘orbital–orbital’’/‘‘lone pair-orbital’’ overlap.

NBO analysis of compound 3a showed that intramolecular charge transfer is:

(i) from π(C1-C4) to π*(C2-O13) with stabilization energy of 20.95 kJ/mol.

(ii) from π(C5-C7) to π*(C1 -C4) and π*(C6- C8) antibonding orbitals with stabilization energy of 20.67 and 19.36 kJ/mol.

(iii) From π(C6-C8) to π*(C5 -C7)and π*(C9-C10) with 16.97 and 19.61 kJ/mol.

(iv) From π(C9-C10) to π*(C5- C7)and π*(C6-C8) with 20.02 and 17.67 kJ/mol.

(v) The magnitude of energy transferred from LP (1) of N11 to π*(C2-O13) and π*(C3-O14) had the stabilization energies 53.85 and 58.49 kJ/mol.

(vi) Similarly, the electron donated from LP(2) of O15 to π*(C6-C8) leads to the stabilization energy of 29.52 kJ/mol.

(vii) Similarly, the electron donated from LP(2) of O16 to π*(C9-C10) leads to the stabilization energy of 28.31 kJ/mol.

NBO analysis of compound 3b showed that intramolecular charge transfer is:

(i) From N_4 of n_1 (N_4) →Π*(C_2-O_{20}) with stabilization energy of 53.94 kcal mol^{-1}.

(ii) From N_4 of n_1 (N_4) to Π*(C_3-O_{19}) with stabilization energy of 58.57 kcal mol^{-1} and 55.05 kcal mol^{-1}.

(iii) The magnitude of energy transferred from O_{19} of n (O_6) to σ* (C_3-S_5) had stabilization energy of 34.41 kcal mol^{-1}.

(iv) Similarly, the electron donated from O_{20} of n (O_{20}) →Π*(C_2-N4) leads to the stabilization energy of 27.76kcal mol^{-1}.

NBO analysis of compound 3c showed that intramolecular charge transfer is:

(i) From N_{15} of n_1 (N_{15}) →Π*(C_{11}-C_{14}) with stabilization energy of 53.01 kcal mol^{-1}.

(ii) From N_5 of n_1 (N_5) to Π*(C_3-O_6) and Π*(C_2-O_7) with stabilization energy of 64.73 kcal mol^{-1} and 55.05 kcal mol^{-1} respectively.

(iii) The magnitude of energy transferred from O_6 of n (O_6) to σ* (C_3-S_4) had stabilization energy of 32.17 kcal mol^{-1}. Similarly, the electron donated from S_4 of n (S_4) →Π*(C_3-C_6) leads to the stabilization energy of 29.66 kcal mol^{-1}.

4.7 Nonlinear optical analysis

Nonlinear optics deals with the interaction of applied electromagnetic fields in various materials to generate new electromagnetic fields, altered in

Table 5(a) — Second order perturbation theory analysis of Fock matrix in NBO basis of the compound 3a.

Donor(i)	Type	ED/e	Acceptor(j)	Type	ED/e	E(2)[a]	E(j)-E(i)[b]	F(i,j)[c]
C1-C4	π	1.8443	C2-O13	Π*	0.30083	20.95	0.29	0.072
C1-C4	π	1.8443	C5-C7	Π*	0.39701	8.9	0.33	0.051
C1-S12	σ	1.96818	C4-C5	σ*	0.02529	5.49	1.12	0.07
C4-H17	σ	1.97094	C5-C7	σ*	0.02397	5.16	1.09	0.067
C5-C7	π	1.61789	C1-C4	Π*	0.0172	20.67	0.26	0.068
C5-C7	π	1.61789	C6-C8	Π*	0.349	19.36	0.27	0.065
C6-C8	π	1.68775	C5-C7	Π*	0.39701	16.97	0.3	0.065
C6-C8	π	1.68775	C9-C10	Π*	0.40323	19.61	0.28	0.068
C7-C9	π	1.97388	C10-O16	Π*	0.02833	5.33	1.04	0.067
C9-C10	π	1.67508	C5-C7	Π*	0.39701	20.02	0.3	0.071
C9-C10	π	1.67508	C6-C8	Π*	0.349	17.67	0.3	0.065
O15-H24	σ*	1.98783	C6-C8	σ*	0.02027	5.61	1.32	0.077
N11	n	1.64475	C2-O13	Π*	0.30083	53.85	0.28	0.111
N11	n	1.64475	C3-O14	Π*	0.3284	58.49	0.27	0.113
O15	n	1.8688	C6-C8	Π*	0.349	29.52	0.34	0.095
O16	n	1.95674	C9-C10	Π*	0.02676	7.26	1.13	0.081
O16	n	1.84634	C9-C10	Π*	0.40323	28.31	0.35	0.095
O16	n	1.84634	H21-C26	σ*	0.01792	5.09	0.75	0.057
C1-C4	π	0.22294	C5-C7	Π*	0.39701	115.86	0.02	0.076
C2-O13	π	0.30083	C1-C4	Π*	0.0172	87.52	0.02	0.076
C9-C10	π	0.40323	C5-C7	Π*	0.39701	210.05	0.02	0.083
C9-C10	π	0.40323	C6-C8	Π*	0.349	304.85	0.01	0.082

[a] E(2) means energy of hyperconjugative interactions (stabilization energy in Kcal/mol)
[b] Energy difference between donor and acceptor i and j NBO orbitals in a.u.
[c] F(ij) is the Fock matrix elements between i and j NBO orbitals in a.u.

Table 5(b) — Second order perturbation theory analysis of Fock matrix in NBO basis of the compound 3b.

Donor(i)	Type	ED/e	Acceptor(j)	Type	ED/e	E(2)	E(j)-E(i)	F(i,j)
C1-C7	π	1.84336	C2-O20	π *	0.30325	21.17	0.29	0.072
C1-C7	π	1.84336	C8-C10	π *	0.39044	8.75	0.32	0.051
C7-H18	σ	1.9709	C1-C2	σ*	0.07649	7.83	0.94	0.077
C7-H18	σ	1.9709	C8-C10	σ*	0.02455	5.33	1.09	0.068
C8-C10	π	1.59812	C1-C7	π *	0.22958	21.78	0.26	0.07
C8-C10	π	1.59812	C9-C12	π *	0.28936	21.2	0.28	0.07
C8-C10	π	1.59812	C11-C13	π *	0.39609	17.5	0.26	0.061
C9-C12	π	1.72106	C8-C10	π *	0.02455	14.42	0.29	0.06
C9-C12	π	1.72106	C11-C13	π *	0.39609	21.68	0.28	0.072
C11-C13	π	1.62382	C8-C10	π *	0.02455	24.87	0.29	0.076
C11-C13	π	1.62382	C9-C12	π *	0.28936	14.97	0.29	0.06
N4	n	1.64475	C2-O20	π *	0.30325	53.94	0.28	0.11
N4	n	1.64475	C3-O19	π *	0.32889	58.57	0.27	0.113
S5	n	1.77793	C1-C7	π *	0.22958	15.81	0.27	0.059
S5	n	1.77793	C3-O19	σ*	0.32889	28.53	0.24	0.076
O19	n	1.81077	C3-N4	σ*	0.08663	26.1	0.67	0.122
O19	n	1.81077	C3-S5	σ*	0.12148	34.41	0.41	0.108
O20	n	1.85276	C1-C2	σ*	0.07649	19.33	0.68	0.104
O20	n	1.85276	C2-N4	σ*	0.08064	27.76	0.67	0.124
O21	n	1.96397	C11-C13	π *	0.02928	7.62	1.1	0.082
O21	n	1.82219	C11-C13	π *	0.39609	32.9	0.34	0.1
O21	n	1.82219	C22-H23	σ*	0.01841	5.22	0.74	0.058
O21	n	1.82219	C22-H25	σ*	0.01841	5.22	0.71	0.058

[a] E(2) means energy of hyperconjugative interactions (stabilization energy in Kcal/mol)
[b] Energy difference between donor and acceptor i and j NBO orbitals in a.u.
[c] F(ij) is the Fock matrix elements between i and j NBO orbitals in a.u.

Table 5(c) — Second order perturbation theory analysis of Fock matrix in NBO basis of the compound 3c.

Donor(i)	Type	ED/e	Acceptor(j)	Type	ED/e	E(2)[a]	E(j)-E(i)[b]	F(i,j)[c]
C1-S4	σ	1.968	C8-C9	σ^*	0.0248	5.27	1.15	0.069
C1-C8	π	1.826	C2-O7	π^*	0.3346	23.99	0.28	0.076
C1-C8	π	1.826	C9-C10	π^*	0.4538	8.52	0.31	0.05
C8-H19	σ	1.97	C9-C12	σ^*	0.0258	5.72	1.08	0.07
C9-C10	π	1.591	C1-C8	π^*	0.2701	27.76	0.26	0.08
C9-C10	π	1.59	C11-C14	π^*	0.4514	16.86	0.26	0.06
C11-C14	π	1.56	C9-C10	π^*	0.4538	29.49	0.27	0.08
C11-C14	π	1.56	C12-C13	π^*	0.2684	12.92	0.29	0.057
C12-C13	π	1.742	C9-C10	π^*	0.4538	13.45	0.28	0.058
S4	n	1.78	C3-O6	π^*	0.3596	29.66	0.24	0.077
N5	n	1.63	C2-O7	π^*	0.3346	55.05	0.27	0.11
N5	n	1.63	C3-O6	π^*	0.3596	64.73	0.26	0.115
O6	n	1.82	C3-S4	σ^*	0.114	32.17	0.42	0.106
N15	n	1.667	C11-C14	π^*	0.4514	53.01	0.26	0.108

[a] E(2) means energy of hyperconjugative interactions (stabilization energy in Kcal/mol)
[b] Energy difference between donor and acceptor i and j NBO orbitals in a.u.
[c] F(ij) is the Fock matrix elements between i and j NBO orbitals in a.u.

Table 6 — Dipole moment μ, polarizability α_{tot} ($\times 10^{-24}$ esu) and first order static hyperpolarizability β_{tot} (10^{-30}) data for (3a-c) calculated at DFT/B3LYP /6-31G(d,p) level of theory.

Dipole moment	3a	3b	3c	Hyper polarizability	3a	3b	3c
μ_x	5.5203	4.6573	9.9143	β_{xxx}	-15.5044	-0.13395	-132.169
μ_y	2.3722	0.6412	0.0383	β_{xxy}	0.74197	0.00641	-0.24028
μ_z	0.1576	0.0004	0.2297	β_{xyy}	-1.6666	-0.0144	-0.52578
μ	6.0105	4.7012	9.917	β_{yyy}	0.84674	0.007315	0.245337
Polarizability							
α_{xx}	47.86371	7.093402	82.8106	β_{xxz}	0.002592	2.24E-05	0.005637
α_{xy}	0.435501	0.064541	-0.87952	β_{xyz}	-0.00338	-2.9E-05	0.00795
α_{yy}	22.21874	3.292817	32.78955	β_{yyz}	-0.00598	-5.2E-05	0.00792
α_{xz}	-0.00011	-1.6E-05	0.002094	β_{xzz}	0.110834	0.000958	0.729153
α_{yz}	-0.00021	-3.1E-05	-0.00419	β_{yzz}	0.199813	0.001726	-0.12742
α_{zz}	9.183228	1.360954	13.25502	β_{zzz}	-0.00027	-2.3E-06	0.005066
<α>	79.26567	3.915724	42.95172	$\beta_{total(esu)}$	17.1536	15.7605	131.96

wavenumber, phase, or other physical properties[61]. Organic molecules able to manipulate photonic signals efficiently are of importance in technologies such as optical communication, optical computing, and dynamic image processing[62,63]. Organic materials have been shown in recent years to possess superior second-order nonlinear optical properties compared to the more traditional inorganic materials. This property together with the inherent ultra-fast response time and enumerable structural variations of organic materials has drawn a sizeable amount of research interest in organic nonlinear optical (NLO) materials. In this context, the first hyperpolarizability was also calculated in the present study. First hyper-polarizability is a third rank tensor that can be described by a 3×3×3 matrix. The 27 components of the 3D matrix can be reduced to 10 components due to the Kleinman symmetry[64].

Since the value of the polarizabilities α and the hyperpolarizability of Gaussion output is reported in a atomic mass units (a.u.), the calculated values have been converted into electrostatic units (esu) (α: 1 a.u = 0.1482×10^{-24} esu; β: 1 a.u. = $.0086393\times10^{-30}$ esu). The results of electronic dipole moment μi (i = x, y, z), polarizability αij and first order hyperpolarizability[65] βijk are listed in Table 6. The calculated first hyper polarizability values of the all the three compounds are greater than that of the standard NLO material urea[66] (0.13×10^{-30} esu), concluding that all the three compounds can be used as nonlinear optical material. Urea is the classical molecule used in the study of the NLO properties of the molecular systems and is used

often as a threshold value for comparative purposes. The dipole moment of 3a/3b/3c is calculated to be 6.0105/4.7012/9.917 Debye with maximum contribution from X direction. In Y and Z directions, dipole moment is practically negligible. The calculated dipole moment for three molecules is given in Table 6. Table 6 shows that the calculated values of a dipole moment in case of 3a and 3b are nearly equal and quite lower than 3c. The first static hyperpolarisability value is found to be appreciably higher 131.96×10^{-30} in 3c than 3a and 3b.

4.8 Thermodynamic properties

Several thermodynamic parameters like zero-point vibrational energy, rotational constants, thermal energy and rotational temperatures of studied molecules have been calculated using DFT / B3LYP functional with 6 31-G(d,p) basis set (Table 7). On the basis of vibrational analysis and statistical thermodynamics, the standard thermodynamic functions such as heat capacity (CV) and entropy (S) for the title molecules were calculated from 100 to 500 K and are listed in Table 8. As seen from the table, standard thermodynamical parameters increase with an increase in temperature, which is attributed to the enhancement of molecular vibration with the temperature[67,68]. The corresponding fitting equations and correlation values are given in Table 9 and the correlation graphics are shown in Fig. 8.

4.9 Chemical reactivity

4.9.1 Global reactivity descriptors

Global reactivity descriptors such as HOMO & LUMO, band gap ($\varepsilon_{LUMO} - \varepsilon_{HOMO}$), ionization potential (I), electron affinity (A), electronegativity (χ), global hardness (η), chemical potential (μ), global electrophilicity index (ω), global softness (S) and additional electronic charge (ΔN_{max}) of reactant A, B and product C for compound 3a, 3b and 3c have been calculated[65] and are listed in Table 10.

Table 7 — Calculated thermodynamic parameters of compounds 3(a-c).

Parameters	3a	3b	3c
Zero-point vibrational energy (Kcal/mol)	118.0423	115.4854	140.8308
Rotational temperature (K)	0.6087	0.07769	0.07161
	0.00822	0.00908	0.00766
	0.00725	0.00814	0.00693
Rotational Constant (GHZ) X	1.26839	1.61872	1.49212
Y	0.17127	0.18925	0.15953
Z	0.15104	0.16962	0.14439
Total Energy E_{total} (Kcal/mol)	127.666		150.883
Transational	0.889	0.889	0.889
Rotational	0.889	0.889	0.889
Vibrational	125.888	122.536	149.106

Table 8 — Thermodynamic functions at different temperatures at the B3LYP /6-31-G (d,p) level.

Temperature (T) (K)	Heat capacity(CV) (Cal/mol K)			Entropy (S) (Cal/mol K)		
	3a	3b	3c	3a	3b	3c
100	23.76	21.961	25.669	83.77	81.519	86.657
200	41.48	37.653	42.675	107.094	102.896	111.021
298.15	57.63	52.932	59.351	127.515	121.599	131.979
300	57.918	53.21	59.658	127.885	121.94	132.359
400	72.301	67.239	75.404	147.145	139.79	152.295
500	84.222	78.976	88.885	165.048	156.542	171.059

Table 9 — Correlation values and correlation equations of compounds 3(a-c) using B3LYP /6- 31G (d, p).

S. No.	Compound	Correlation equations		Correlation values	
		Heat capacity(CV)	Entropy (S)	(CV)	(S)
1	3a	$CV = 3.5731 + 0.2104T - 1.10^{-5}T^2$	$S = 59.255 + 0.2553T - 9.10^{-5}T^2$	0.99	1
2	3b	$CV = 3.9816 + 0.1843T - 7.10^{-5}T^2$	$S = 59.278 + 0.2312T - 7.10^{-5}T^2$	0.99	1
3	3c	$CV = 6.5645 + 0.1947T - 6.10^{-5}T^2$	$S = 61.413 + 0.2635T - 9.10^{-5}T^2$	0.99	0.99

It has been found that compound 3b is harder (more stable) than 3a and 3c as its calculated binding energy and chemical hardness has higher values. The chemical potential characterizes the tendency of an electron to escape from the molecule in the equilibrium state. In the present work, the chemical potential varies with the substituent present on the aromatic ring and found to be higher for 3b while global electrophilicity index decreases from 3a to 3c.

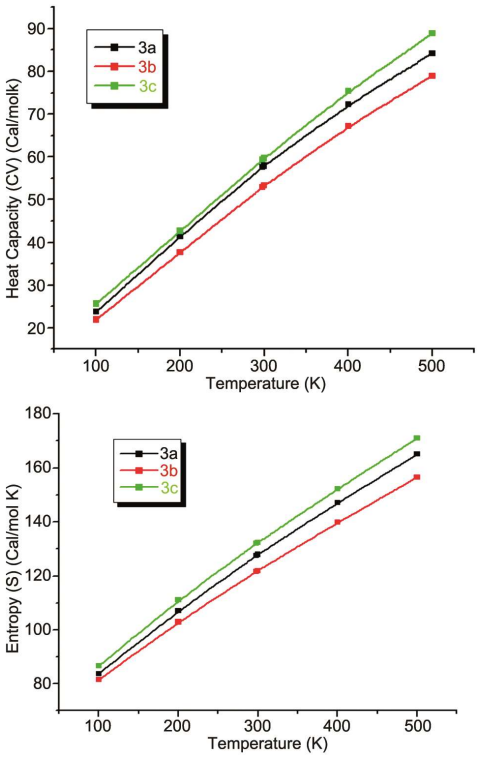

Fig. 8 — Correlation graphs of heat capacity and entropy calculated at various temperatures using B3LYP.

Electrophilic charge transfer[65] (ECT) is defined as the difference between the ΔN_{max} values of interacting molecules. If we consider two molecules A and B approach to each other (i) if ECT > 0, charge flow from B to A (ii) if ECT < 0, charge flow from A to B.

The calculated value of ECT < 0 (ECT = -0.2693, -0.4702 and -1.544 for 3a, 3b and 3c), for reactant molecules thiazolidine- 2, 4-dione (1) and substituted benzaldehyde (2) indicates charge flow from reactant 1 to reactant 2. Therefore, in all cases the reactant molecule (1) acts as global nucleophile (electron donor) and (2) as global electrophile (electron acceptor).

4.9.2 Local reactivity descriptors

Using Hirshfeld population analysis of neutral, cation and anion state of molecule, Fukui Functions are calculated. Fukui functions (f_k^+, f_k^-), local softnesses (s_k^+, S_k^-) and local electrophilicity indices[65] (ω_k^+, ω_k^-) for selected atomic sites of molecule have been listed in Table 11 which shows that the relative high values of local reactivity descriptors (f_k^+, s_k^+, ω_k^+):

(i) At C2 indicates that this site is prone to nucleophilic, whereas the relatively high values of local reactivity descriptors at O13 indicate that this site is more prone to electrophilic attack for compound 3a.

(ii) At C2 indicates that this site is prone to nucleophilic, whereas the relatively high values of local reactivity descriptors at O20 indicate that this site is more prone to electrophilic attack for compound 3b.

(iii) At C2 indicates that this site is prone to nucleophilic, whereas the relatively high values of local reactivity descriptors at O7 indicate that this site is more prone to electrophilic attack for compound 3c.

Table 10 — Calculated ε_{LUMO}, ε_{HOMO}, energy band gap $\varepsilon_{LUMO} - \varepsilon_{HOMO}$, ionization potential (IP), electron affinity (EA), electronegativity (χ), global hardness (η), chemical potential (μ), global electrophilicity index (ω), global softness (S) and additional electronic charge (ΔN_{max}) in eV for 3(a-c) using B3LYP/6-31G(d,p).

	ε_H	ε_L	ε_H-ε_L	I	A	χ	η	μ	ω	S	ΔN_{max}
3a											
Reactant (A)	-7.42	-1.06	-6.36	7.42	1.06	4.24	3.18	-4.24	2.83	0.15	1.33
Reactant (B)	-6.04	-1.4	-4.64	6.04	1.4	3.72	2.32	-3.72	2.98	0.21	1.6
Product (C)	-5.73	-2.19	-3.54	5.73	2.19	3.96	1.77	-3.96	4.43	0.28	2.23
3b											
Reactant (A)	-7.429	-1.063	-6.365	7.429	1.063	4.246	3.182	-4.246	2.83	0.157	1.33
Reactant (B)	-4.36	-1.24	-3.12	4.36	1.24	2.8	1.56	-2.8	2.52	0.32	1.8002
Product (C)	-5.83	-2.19	-3.64	5.8394	2.1953	4.0173	1.822	-4.01	4.428	0.2744	2.2048
3c											
Reactant (A)	-5.692	-1.931	3.76	5.692	1.931	-3.811	1.88	3.8115	3.86	0.265	-2.027
Reactant (B)	-5.493	-1.069	4.42	5.493	1.0699	-3.281	2.2115	3.2814	2.434	0.226	-1.483
Product (C)	-5.253	2.0359	-3.21	5.2533	2.0359	-3.685	1.608	3.6446	4.128	0.3108	-2.26

Table 11 — Using Hirshfeld population analysis: Fukui functions (f_k^+,f_k^-), Local softnesses (sk^+, sk^-) in eV, local electrophilicity indices (ωk^+, ωk^-) in eV for selected atomic sites of product.

	Hirshfeld atomic charges			Fukui functions		Local softnesses		Local electrophilicity indices	
	q_N	q_N+1	q_N-1	f_k+	f_k-	sk^+	sk^-	ω_k^+	ω_k^-
3a									
1C	-0.17571	-0.20245	-0.25209	-0.02675	0.076389	-0.00755	0.021549	-0.11869	0.338984
2C	0.484585	0.646914	0.543502	0.162329	-0.05892	0.045793	-0.01662	0.720351	-0.26145
3C	0.364807	0.442836	0.404743	0.078029	-0.03994	0.022012	-0.01127	0.346261	-0.17722
4C	0.007674	0.043787	-0.16741	0.036113	0.17508	0.010187	0.04939	0.160255	0.776935
5C	0.117284	0.143875	0.146475	0.026591	-0.02919	0.007501	-0.00823	0.118	-0.12954
6C	-0.07887	0.01667	-0.13252	0.095541	0.053651	0.026952	0.015135	0.423973	0.238082
7C	-0.18368	0.104957	-0.04564	0.288637	-0.13804	0.081424	-0.03894	1.280856	-0.61256
8C	0.265799	0.323802	0.270859	0.058003	-0.00506	0.016363	-0.00143	0.257394	-0.02245
9C	-0.07162	0.031623	-0.10554	0.103243	0.033918	0.029125	0.009568	0.458151	0.150515
10C	0.307497	0.393141	0.282161	0.085644	0.025336	0.02416	0.007147	0.380054	0.112431
11N	-0.19573	-0.21187	-0.29936	-0.01614	0.103627	-0.00455	0.029233	-0.07162	0.459855
12S	0.270983	0.364472	0.076838	0.093489	0.194145	0.026373	0.054768	0.414867	0.861538
13O	-0.09766	-0.44962	-0.57237	-0.35197	0.474716	-0.09929	0.133917	-1.5619	2.1066
14O	-0.44549	-0.38665	-0.53656	0.05884	0.091064	0.016599	0.025689	0.261108	0.404106
15O	-0.25386	-0.13931	-0.28294	0.114551	0.029077	0.032315	0.008203	0.508332	0.129032
16O	-0.54668	-0.50195	-0.57253	0.044731	0.025855	0.012619	0.007294	0.198498	0.114734
26C	0.230664	0.379778	0.242379	0.149114	-0.01172	0.042065	-0.0033	0.661708	-0.05199
3b									
1 C	-0.17467	-0.19825	-0.24921	-0.02358	0.07454	-0.00647	0.020454	-0.10445	0.330125
2 C	0.484033	0.647908	0.542051	0.163875	-0.05802	0.044967	-0.01592	0.725775	-0.25695
3 C	0.364736	0.442377	0.404722	0.077641	-0.03999	0.021305	-0.01097	0.343859	-0.17709
4 N	-0.19574	-0.20883	-0.29887	-0.01309	0.103131	-0.00359	0.028299	-0.05796	0.45675
5 S	0.268804	0.382172	0.074727	0.113368	0.194077	0.031108	0.053255	0.502088	0.859534
7 C	0.002873	0.04582	-0.17305	0.042947	0.175922	0.011785	0.048273	0.190205	0.779129
8 C	0.127011	0.152712	0.149336	0.025701	-0.02233	0.007052	-0.00613	0.113825	-0.09887
9 C	-0.0783	0.034409	-0.10675	0.112713	0.028442	0.030928	0.007804	0.499187	0.125965
10 C	-0.18592	0.087702	-0.04179	0.273623	-0.14413	0.075082	-0.03955	1.21183	-0.63832
11 C	-0.06345	0.041127	-0.10506	0.104577	0.041606	0.028696	0.011417	0.463154	0.184266
12 C	-0.0222	0.080209	-0.08777	0.102407	0.065568	0.0281	0.017992	0.453543	0.29039
13 C	0.363474	0.392396	0.308862	0.028922	0.054612	0.007936	0.014986	0.128091	0.241867
19 O	-0.44656	-0.38151	-0.53645	0.06505	0.089889	0.01785	0.024666	0.288095	0.398103
20 O	-0.0945	-0.44329	-0.573	-0.34879	0.478506	-0.09571	0.131302	-1.54474	2.119222
21 O	-0.56672	-0.44422	-0.53423	0.122492	-0.03248	0.033612	-0.00891	0.542496	-0.14387
22 C	0.217126	0.369271	0.226478	0.152145	-0.00935	0.041749	-0.00257	0.673824	-0.04142
3c									
1C	-0.18233	-0.19774	-0.25002	-0.0154	0.067684	-0.00479	0.021036	-0.06358	0.2794
2C	0.493967	0.640279	0.539698	0.146312	-0.04573	0.045474	-0.01421	0.603976	-0.18878
3C	0.363305	0.44224	0.404224	0.078935	-0.04092	0.024533	-0.01272	0.325844	-0.16891
4S	0.263046	0.331103	0.070437	0.068057	0.192609	0.021152	0.059863	0.280939	0.79509
5N	-0.19966	-0.21804	-0.30016	-0.01837	0.100494	-0.00571	0.031234	-0.07584	0.414839
6O	-0.44764	-0.39858	-0.53972	0.049055	0.092087	0.015246	0.028621	0.202499	0.380135
7O	-0.10322	-0.4553	-0.57635	-0.35208	0.473132	-0.10943	0.147049	-1.45339	1.953089
8C	0.00234	0.018851	-0.17639	0.016511	0.178732	0.005132	0.05555	0.068157	0.737806
9C	0.125257	0.160367	0.154683	0.03511	-0.02943	0.010912	-0.00915	0.144934	-0.12147
10C	-0.08252	0.011815	-0.12677	0.094333	0.04425	0.029319	0.013753	0.389407	0.182664
11C	-0.05506	0.038687	-0.11223	0.09375	0.057166	0.029138	0.017767	0.387	0.235981
12C	-0.23801	0.067291	-0.04374	0.305299	-0.19427	0.094887	-0.06038	1.260274	-0.80196
13C	-0.02837	0.032434	-0.10851	0.060806	0.080139	0.018899	0.024907	0.251007	0.330814
14C	0.315689	0.365707	0.316864	0.050018	-0.00117	0.015546	-0.00037	0.206474	-0.00485
15N	-0.52076	-0.44889	-0.50954	0.07187	-0.01122	0.022337	-0.00349	0.296679	-0.04632
16C	0.110933	0.303926	0.126	0.192993	-0.01507	0.059982	-0.00468	0.796675	-0.0622
17C	0.183033	0.305841	0.131513	0.122808	0.05152	0.038169	0.016012	0.506951	0.212675

Table 12 — Geometrical parameters (bond length) and topological parameters for bonds of interacting atoms: electron density (ρBCP), Laplacian of electron density $\nabla^2\rho$(BCP)), electron kinetic energy density (*G*BCP), electron potential energy density (*V*BCP), total electron energy density (*H*BCP) at bond critical point (BCP) and estimated interaction energy (E_{int}) of compounds (3a-c).

	Interaction	Bond length	ρ (BCP)	∇^2 ρ (BCP)	G(BCP)	V(BCP)	H(BCP)	Elipticity	E_{int} (Kcal/mol)
3a									
1	O13 - H19	2.02	0.02	0.07	0.01	-0.01	-0.0003	0.04	-6.00204
2	O16 - H24	2.09	0.02	0.08	0.01	-0.01	0.001388	0.115	-5.6064
3b									
1	H17 - O20	2.03	0.02	0.07	0.02	-0.02	-0.003	0.01	-6.03
3c									
10	O7 - H22	2.035	0.024182	0.072622	0.018488	-0.0188	-0.00033	0.006293	-5.90509

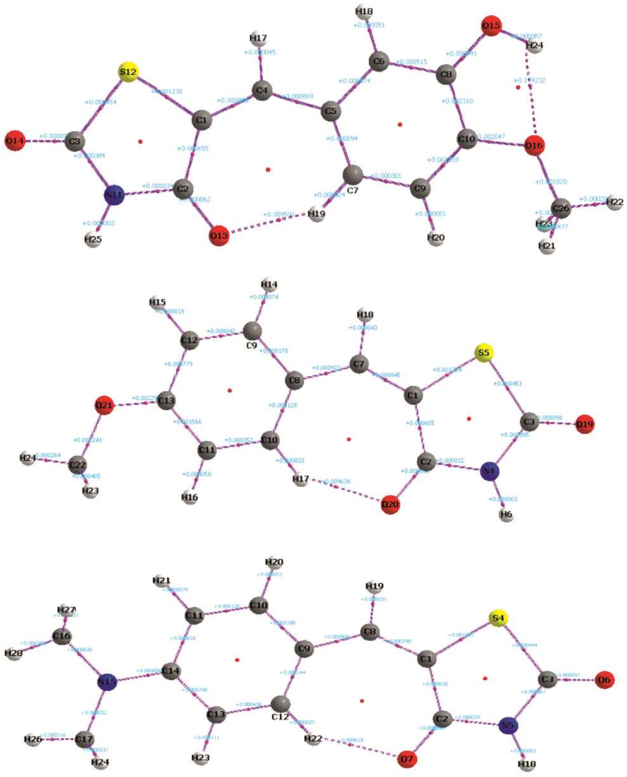

Fig. 9 — Molecular graph of the compounds(3a-c) using AIM program at B3LYP/6- 31G (d,p) level.

4.10 AIM approach

Molecular graph of the compounds using AIM program at B3LYP/6- 31G (d,p) level is presented in Fig. 9. According to Rozas *et al.*[69] the interactions may be classified as follows:

(i) Strong H-bonds are characterized by $\nabla^2\rho$(BCP) < 0 and *H*BCP < 0 and their covalent character is established.

(ii) Medium H-bonds are characterized by $\nabla^2\rho$ (BCP) > 0 and *H*BCP < 0 and their partially covalent character is established.

(iii) Weak H-bonds are characterized by $\nabla^2\rho$(BCP) > 0 and *H*BCP > 0 and they are mainly electrostatic (where, ρ(BCP) and *H*BCP are Laplacian of electron density and total electron energy density at bond critical point respectively) and the distance between interacting atoms is greater than the sum of Van der Waal's radii of these atoms.

Geometrical as well as topological parameters for bonds of interacting atoms are given in Table 12, according to above criteria:

(i) The interactions O13….H19, are medium and the interaction O16….H24 is weak interaction for compound 3a and as all ∇^2(BCP) and *H*BCP parameters were greater than zero hence H17 - O20 are weak interactions in case of compound 3b and O7…H22 are weak interactions in case of compound 3c.

Bader's theory application was used to estimate hydrogen bond energy (*E*). Espinosa proposed proportionality between hydrogen bond energy (*E*) and potential energy density[70] (VBCP): $E = 1/2(VBCP)$. According to AIM calculation, the total energy of intramolecular interactions was calculated as -11.6084, -6.03 and -5.90 kcal/mol for 3a, 3b and 3c.

The ellipticity (ε) at BCP is a sensitive index to monitor the π-character of bond. The ε is related to $\lambda 1$ and $\lambda 2$, which corresponds to the eigen values of Hessian and defined by a relationship: $\varepsilon = (\lambda 1/\lambda 2) - 1$. The ellipticity values for bonds are given in Table 12. The lower values of ellipticity confirm that there is delocalization of electrons in aromatic ring[71].

5 Conclusions

The spectroscopic features of compounds 3(a-c) were investigated by combined FT-IR, UV-Vis, ^{1}H, ^{13}C NMR spectroscopic techniques. In the present work, the geometric parameters, the vibrational frequencies, frontier orbital band gap, MESP surfaces and the non-linear optical properties of compound 3a/3b/3c were calculate using DFT/ B3LYP method.

The higher frontier orbital energy gap and the lower dipole moment values make the compound 3b less reactive and less polar, hence most stable among the three molecules. A good agreement between experimental and calculated normal modes of vibrations has been observed. The assignments of wavenumbers were made with PED. The energies of the important molecular orbitals and the electronic absorption wavelengths were also investigated by TD-DFT method along with the other electronic and NLO properties. The thermodynamic features were obtained by DFT/B3LYP. The thermodynamic functions; heat capacity (C) and entropy (S) increase with the increasing temperature (100–500 K) owing to the intensities of the molecular vibrations. The local reactivity descriptors (f_k^-, s_k^-, ω_k^-) indicate the site for electrophilic and nucleophilic attack. The compound 3c has significantly higher value (131.96×10^{-30}) of total hyperpolarizability.

Acknowledgement

The authors express their sincere thanks to the Head, Department of Chemistry, Lucknow University, Lucknow, for providing laboratory facilities. They are also thankful to the Director, CDRI, Lucknow for spectral data. Authors are thankful to Council of Science and Technology, UP, India for financial support.

References

1 Camps M, R€uckle T, Ji H, Ardissone V, Rintelen F, Shaw J, Ferrandi C, Chabert C, Gillieron C, Franc-on B, Martin T, Gretener D, Perrin D, Leroy D, Vitte P A, Hirsch E, Wymann M P, Cirillo R, Schwarz M K & Rommel C, *Nat Med* , 11 (2005) 936.

2 Xia Z, Knaak C, Ma J, Beharry Z M, Mclnnes C, Wang W, Kraft A S & Smith C D, *J Med Chem*, 52 (2009) 74.

3 Katritzky A R, Tala S R, Lu H, Vakulenko A V, Chen Q Y, Sivapackiam J, Pandya K, Jiang S & Debnath A K, *J Med Chem*, 52 (2009) 7631.

4 Heidi S C, *Curr Opin Invest Drugs*, 4 (2003) 406.

5 Blokh G A, Melamed Ch L, Grichshuk A I & Jaroshenko L P, *Chem Abstr*, 66 (1967) 11598.

6 Hirabayashi S, Nagaoka Y & Kokai T K J P, *Chem Abstr*, 117 (1992) 160723.

7 Mifune H, Tani T & Kokai T K J P, *Chem Abstr*, 118 (1993) 29894.

8 Bruno G, Costantino L, C Curinga, R Maccari, F Monforte F Nicolo, R Ottana & Vigorita M G, *Bioorg Med Chem*, 10 (2002) 1077.

9 Y Wu, Karna S, Choi C H, Tong M, Tai H, Dong H N, Jang C H & Cho H, *J Med Chem*, 54 (2011) 5260.

10 Zidar N, Tomasic T, Sink R, Rupnik V, Kovac A, Turk S, Patin D, Blanot D, Martel C C, Dessen A, Premru M M, Zega A, Gobec S, Masic L P & Kikelj D, *J Med Chem*, 53 (2010) 6584.

11 Avupati V R, Yejella R P, Akula A, Guntuku G S, Doddi B R, Vutla V R, Anagani S R, Adimulam L S & Vyricharla A K, *Bioorg Med Chem Lett*, 22 (2012) 6442.

12 Bozdag D O, Verspohl E J, Das E N, Kaup R M, Bauer K, Sarikaya M, Evranos B & Ertan R, *Bioorg Med Chem*, 16 (2008) 6747.

13 Eun J S, Kim K S, Kim H N, Park S A, Ma T, Lee K A, Kim D K, Kim H K, Kim I S, Y H Jung, O P Zee, D J Yoo & Kwak Y G, *Arch Pharm Res*, 30 (2007) 155.

14 Mori M, Takagi M, Noritake C & Kagabu S, *J Pesticide Sci*, 33 (2008) 357.

15 Sahu S K, Banerjee M, Mishra S K & Mohanta R K, *Acta Pol Pharm Drug Res*, 64 (2007) 121.

16 Ragab F A, Eid N M & El-Tawab H A, *Pharmazie*, 52 (1997) 926.

17 Verma A & Saraf S K, *Eur J Med Chem*, 43 (2008) 897.

18 Wanga G, Denga C, Xiea C, Maa L, Yanga J, Qiua N, Xua Q, Chena T, Penga F, Chena J, Qiua J, Penga A, Wei Y & Chena L, *Eur J Med Chem*, 46 (2011) 5941.

19 Baker J, Jarzecki A A & Pulay P, *J Phys Chem*, 102 (1998) 1412.

20 Martin J M L, Alsenoy V & Alsenoy C V, Gar2ped, University of Antwerp, 1995.

21 Zhang Y & Zhou Z, *Organic Chemis Int*, 5 (2012) 194784.

22 Becke A D, *J Chem Phys*, 97 (1992) 9173.

23 Becke A D, *J Chem Phys*, 98 (1993) 5648.

24 Lee C, Yang W & Parr R R, *Phys Rev B*, 37 (1988) 785.

25 Frisch M J, Trucks G W, Schlegal H B, Scuseria G E, Robb M A, Gaussian 09 Rev, Gaussian, Inc, Wallingford CT, 2009.

26 Frisch E, Hratchian H P, Dennington I R D, Keith T A, Millam J, Nielsen A B, Holder A J & Hiscocks J, Gaussian, Inc, Gauss View Version 508, 2009.

27 Ladd M, *Introduction to physical chemistry*, 3rd Edn, (Cambridge University Press), 1998.

28 Allen F H, Kennard O, Watson D G, Brammer L, Orpen A G & Taylor R, *J Chem Soc*, Perkin TransII, (1987) S1-S19.

29 Henryk T, Flakus, Miros A & Jones P G, *J Mol Struct*, 604 (2002) 29.

30 Xiong LY, T F Wang, L P Zheng, Zhanga C & Wang F C, *Acta Cryst E*, 67 (2011) 016.

31 Divjakovic V, Popov-Pergal K, Pergal M & Klement U, *Acta Cryst*, 47 (1991) 1761.

32 Dattagupta J K & Saha N N, *Acta Cryst*, 29 (1973) 1228.

33 Divjakovic V, Popov-Pergal K, Pergal M & Klement U, *Acta Cryst*, 47 (1991) 1760.

34 Sun H S, Yao C H, He W, Tang S G & Guo C, *Acta Cryst*, 63 (2007) 4473.

35 Azizmohammadi M, Khoobi M, Ramazani A, Emami S, Zarrin A, Firuzi O, Miri R & Shafiee A, *Eur J Med Chem*, 59 (2013) 15.

36 Fleming I, *Frontier orbitals and organic chemical reactions*, (John Wiley and Sons: New York, 1976.

37 Foresman J B, Frisch E, *Exploring chemistry with electronic structure methods*, Gaussian, Inc, Pittsburgh, PA, USA, 1993.

38 Gökce H & Bahçeli S, *Spectrochim Acta Part A*, 133 (2014) 741.

39 Bellamy L J, *The infrared spectra of complex molecule*, 3rd Edn, (Wiley: New York), 1975.

40 Anbarasana P M, Subramanian M K, Senthilkumar P, Mohanasundaram C, Ilangovan V & Sundaraganesan N, *J Chem Pharm Res*, 3 (2011) 597.
41 Singh P, Singh N P & Yadav R A, *J Chem Pharm Res*, 3 (2011) 737.
42 Singh R, Kumar M, Singh P & Yadav R A, *J Chem Pharm Res*, 3 (2011) 25.
43 Anbarasan P M, Subramanian M K, Manimegalai S, Suguna K, Ilangovan V, Sundaraganesan N, *J Chem Pharm Res*, 3 (2011) 123.
44 Michalska D, Bienko D C, Bienko A J A, Latajaka Z, *J Phys Chem*, 100 (1996) 17786.
45 Pavia D L, lampman G M & Kris G S, *Introduction to spectroscopy*, 2nd Edn, Harcourt Brace College, (1996) 28.
46 Varsanyi G, *Vibrational spectra of benzene derivatives*, (Academic Press: New York), 1969.
47 Richards R E & Thompson H W, *J Chem Soc*, 47 (1948) 1248.
48 Miyazawa T, *J Mol Spectrosc*, 4 (1960) 155.
49 V Krishnakumar, Manohar S & Nagalakshmi R, *Spectrochim Acta Part A*, 71 (2008) 110
50 Subramanian N, Sundaraganesan N & Jayabharathi J, *Spectrochim Acta Part A*, 76 (2010) 259.
51 Arjunan V, Suja Ravi Isaac A, Rani T, Mythili C V & Mohan S, *Spectrochim Acta Part A,* 78 (2011) 1625.
52 Karabacak M, *J Mol Struct*, 919 (2009) 215.
53 Politzer P & Murray J S, *Theoretical biochemistry and molecular biophysics: A comprehensive survey*, in: Beveridge D L, Lavery R (Eds), Protein, (Academic Press: Schenectady, NY), 1991.
54 Gupta V P, Sharma A, Virdi V & Ram V J, *Spectrochim Acta, Part A*, 64 (2006) 57.
55 Klimentova J, Vojtisek P & Sklenarova M, *J Mol Struct*, 871 (2007) 33.
56 Mulliken R S, *J Chem Phys*, 23 (1955) 1833.
57 Sundaraganesan N, Ilakiamani S, Subramanian P & Joshua B D, *Spectrochim Acta A*, 67 (2007) 628.
58 Krishnakumar V & Ramasamy R, *Spectrochim Acta Part*, 61 (2005) 2526.
59 Szafran M, Komasa A & Adamska E B, *J Mol Struct*, 827 (2007) 101.
60 Glendening E D, Reed A E, Carpenter J E, Weinhold F, NBO Version 31, TCI, University of Wisconsin, Madison, 1998.
61 Shen Y R, *The principles of nonlinear optics*, (Wiley: New York), 1984.
62 Kolinsky P V, *Opt Eng*, 31 (1992) 1676.
63 Eaton D F, *Science,* 25 (1991) 281.
64 Kleinman D A, *Phys Rev*, 126 (1962) 1977.
65 Fatma S, Bishnoi A & Verma A K, *J Mol Struct*, 1095 (2015) 112.
66 Adant M, Dupuis L & Bredas L, *Int J Quantum Chem*, 56 (2004) 497.
67 Bevan Ott J, Boerio-Goates J, *Calculations from statistical thermodynamics*, (Academic Press), 2000.
68 Sajan D, Josepha L, Vijayan N & Karabacak M, *Spectrochim Acta Part A*, 81 (2011) 85.
69 Rozas I, Alkorta I & Elguero J, *J Am Chem Soc*, 122 (2000) 11154.
70 Espinosa E, Molins E & Lecomte C, *Chem Phys Lett*, 285 (1998) 170.
71 Matta L F & Boyd R J, *An introduction of the quantum theory of atom in molecule*, (Wiley-VCH Verlag Gmbh), 2007.